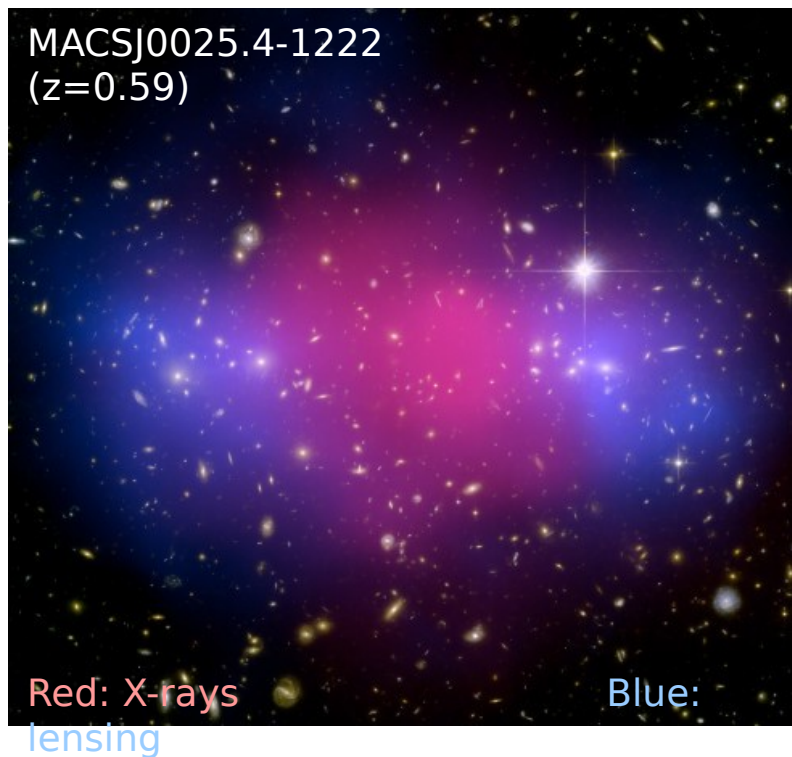


X-rays and the landscape of galaxy cluster astrophysics and cosmology

Steve Allen (Stanford)



In collaboration

with:

Adam Mantz (Stanford)

Douglas Applegate
(Chicago)

Rebecca Canning
(Stanford)

Patrick Kelly (UC
Berkeley)

Anja von der Linden
(SUNY)

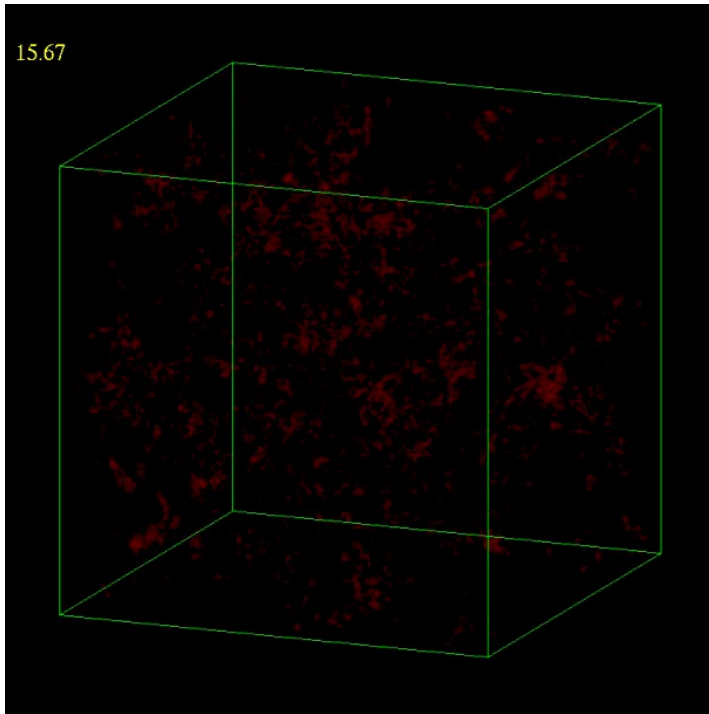
R. Glenn Morris (SLAC)

Ondrej Urban (Stanford)

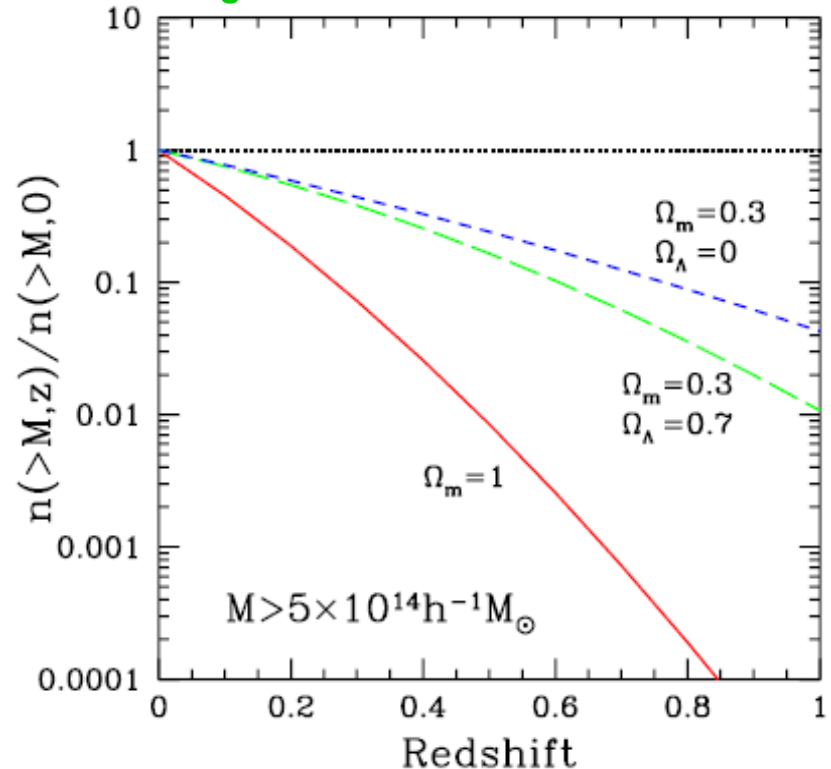
more ...

Cosmology with cluster counts

Moore et al.



Borgani '06



Measurements of the number counts of galaxy clusters, as a function of mass and redshift, provide powerful constraints on cosmological parameters (“... galaxy clusters could emerge as the most powerful cosmological probe”, DOE Cosmic Visions Dark Energy Science report, arXiv:1604.07626)

Ingredients for cluster count experiments

[THEORY] The predicted mass function of clusters, $n(M,z)$, as a function of cosmological parameters (σ_8, Ω_m, w etc).

[CLUSTER SURVEY] A large, clean, complete cluster survey with a well defined selection function.

Current leading catalogs constructed at X-ray (ROSAT), optical (SDSS, DES) and mm (SZ) wavelengths (SPT, ACT, Planck).

[MASS-OBSERVABLE RELATION] Well-calibrated scaling relation linking survey observable (e.g. L_x , richness, SZ flux) and M, z .

Separate into: 1) relative mass calibration
2) absolute mass calibration

(Vikhlinin et al. 2009,
Mantz et al. 2010)

Calibrating cluster masses

X-ray observations

measurements



Relative mass calibration

X-ray measurements provide low-scatter ($<15\%$) mass proxies (M_{gas} , T_x , Y_x) \rightarrow tight relation between survey observable and relative mass.

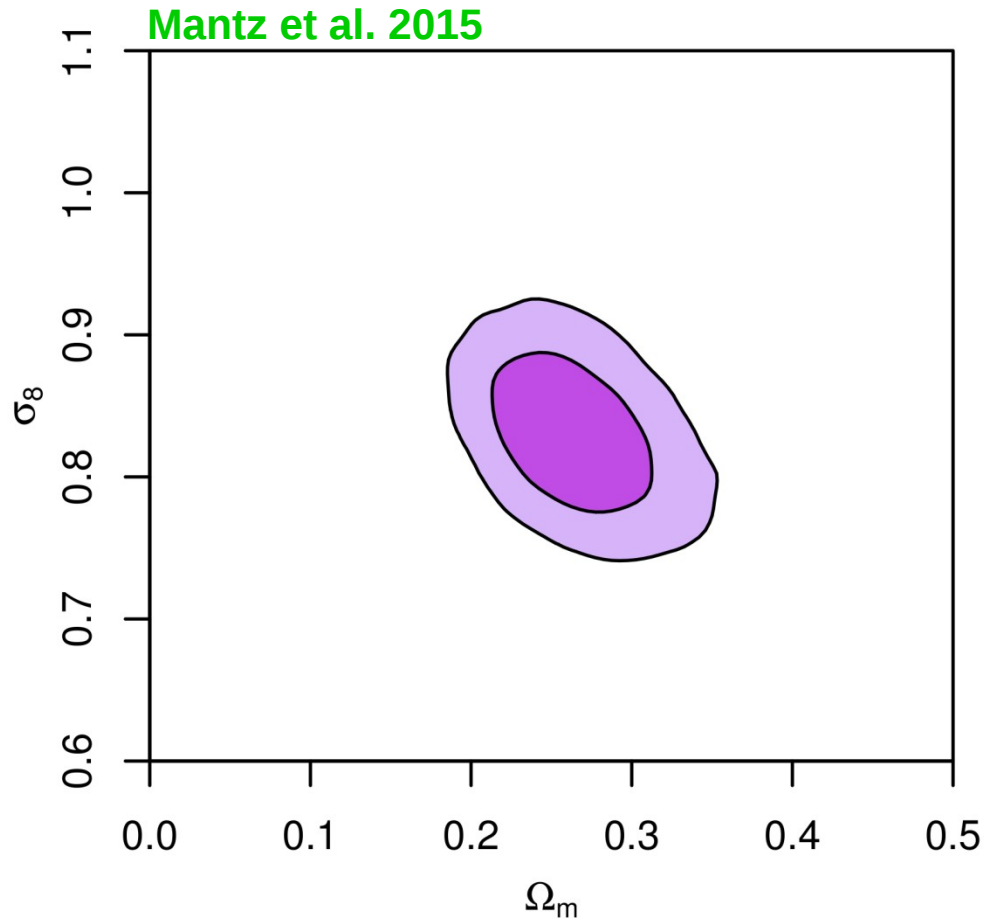
Weak lensing



Absolute mass calibration

WL masses (measured appropriately) are expected to be approximately unbiased on average, with small residual biases being calibratable.

Current constraints (clusters only): σ_8 , Ω_m



Flat Λ CDM model:

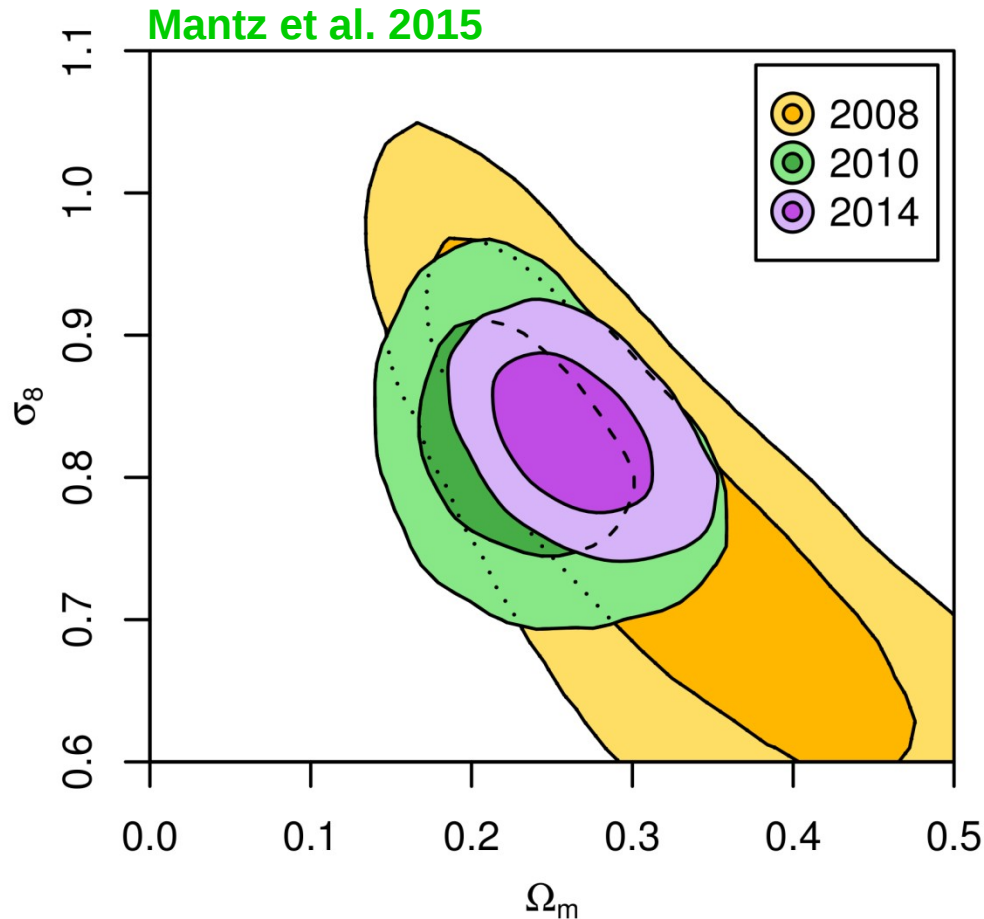
$$\Omega_m = 0.260 \pm 0.030$$
$$\sigma_8 = 0.830 \pm 0.035$$

68% confidence limits,
marginalized over all
systematic uncertainties.
(Standard priors on
 $\Omega_b h^2$ and h included.)

224 ROSAT All-Sky Survey (X-ray) clusters, $z < 0.5$.

+ Chandra X-ray follow-up (139/224) + Weighing the Giants WL (27/224)

The impact of improving mass calibration



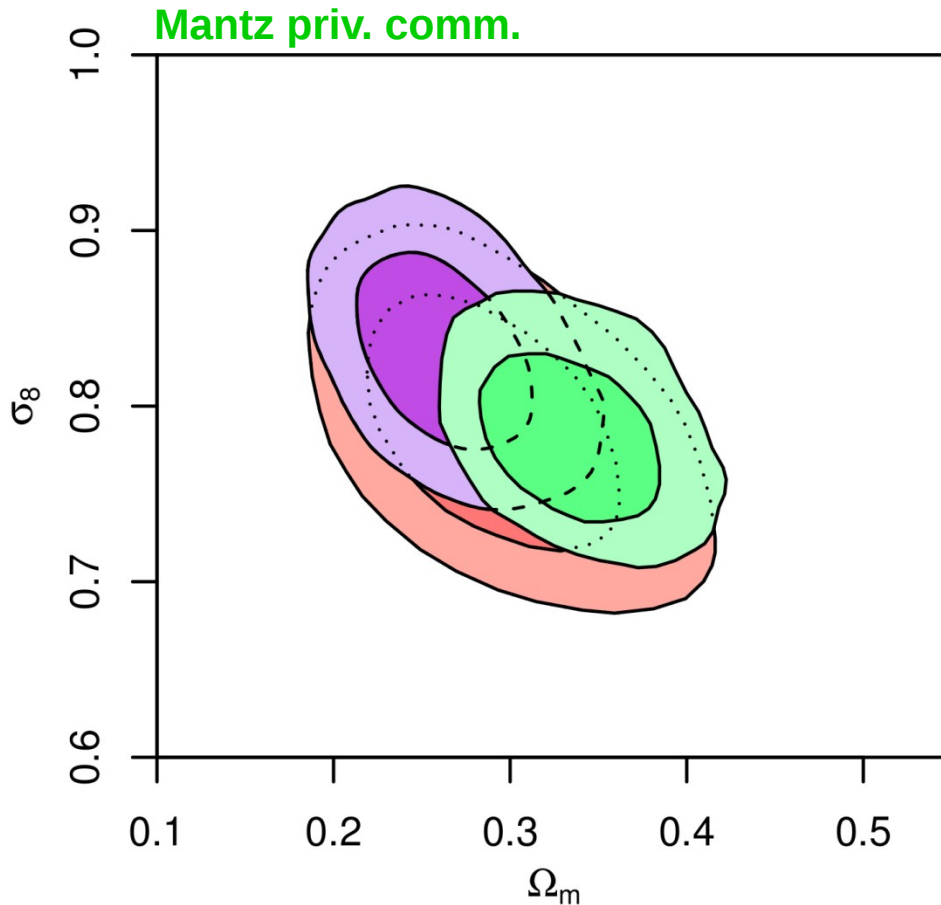
Key advances:

2008→2010: inclusion of low-scatter X-ray mass proxies (+ fgas).

2010→2014: inclusion of Weighing the Giants weak lensing mass calibration.

Addition of Chandra X-ray data + WL mass calibration → substantial boost in cosmological constraining power.

Comparison: X-ray vs. SZ cluster surveys



RASS (+Chandra+WtG)
Planck Clusters (+XMM+WtG)
SPT (+Chandra+WtG/H15)

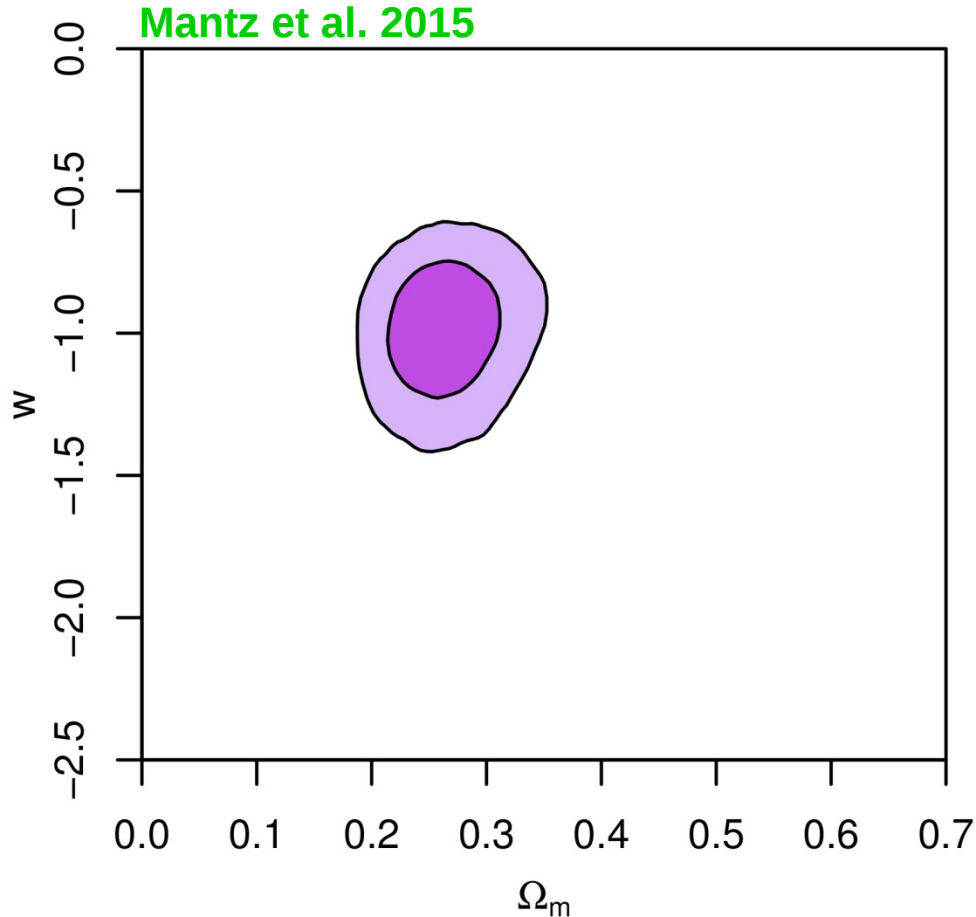
Good agreement between X-ray and SZ cluster counts when employing consistent absolute mass calibration.

Also consistent with earlier X-ray and optical results (Mantz et al '08,'10; Vikhlinin et al '09; Rozo et al '10)

Planck Clusters: Planck Collaboration et al. 2016 (arXiv:1502.01597)

SPT: De Haan et al. 2016 (arXiv:1603.06522)

Results on dark energy (RASS clusters only)



Flat, constant w model:

$$\Omega_m = 0.261 \pm 0.031$$

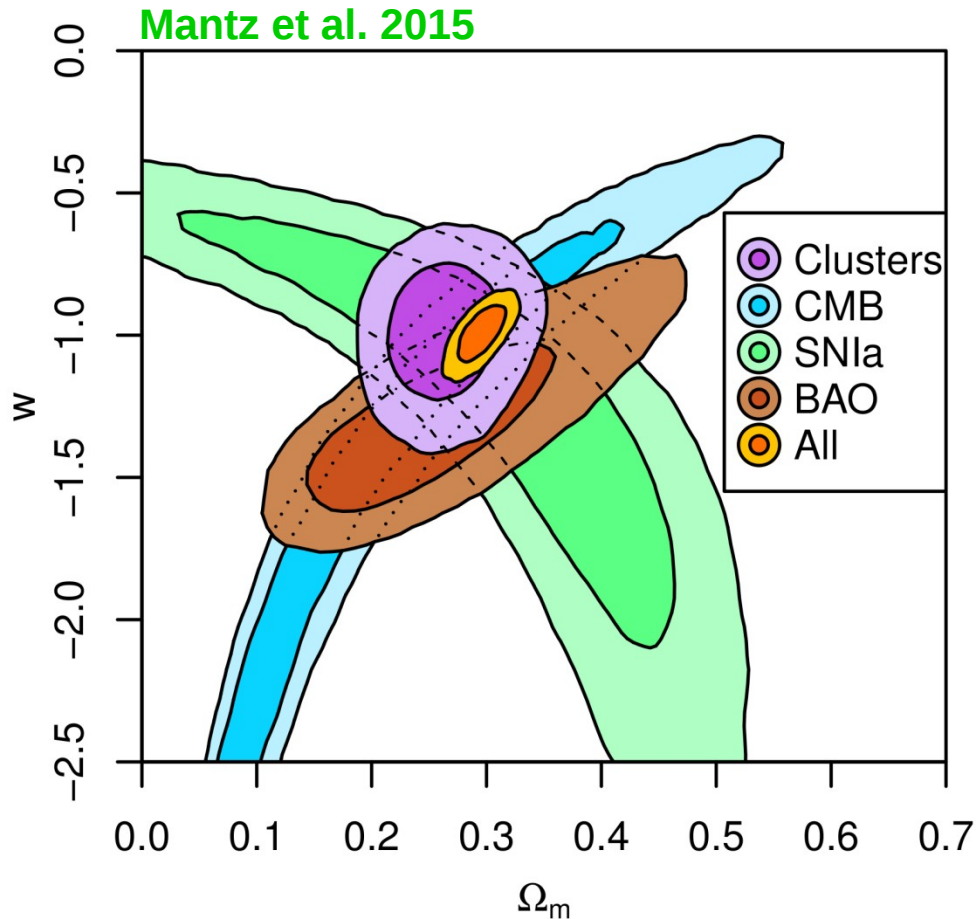
$$\sigma_8 = 0.831 \pm 0.036$$

$$w = -0.98 \pm 0.15$$

68% confidence limits,
marginalized over all
systematic uncertainties.
(Standard priors on
 $\Omega_b h^2$ and h included.)

near detection of the effects of dark energy on cluster growth.

Dark energy: clusters vs. independent techniques



Flat, constant w model:

Clusters (Mantz et al. '15)

CMB (WMAP9+SPT+ACT)

SNIa (Suzuki et al. '12)

BAO (Anderson et al. '14)

Combined constraint (68%)

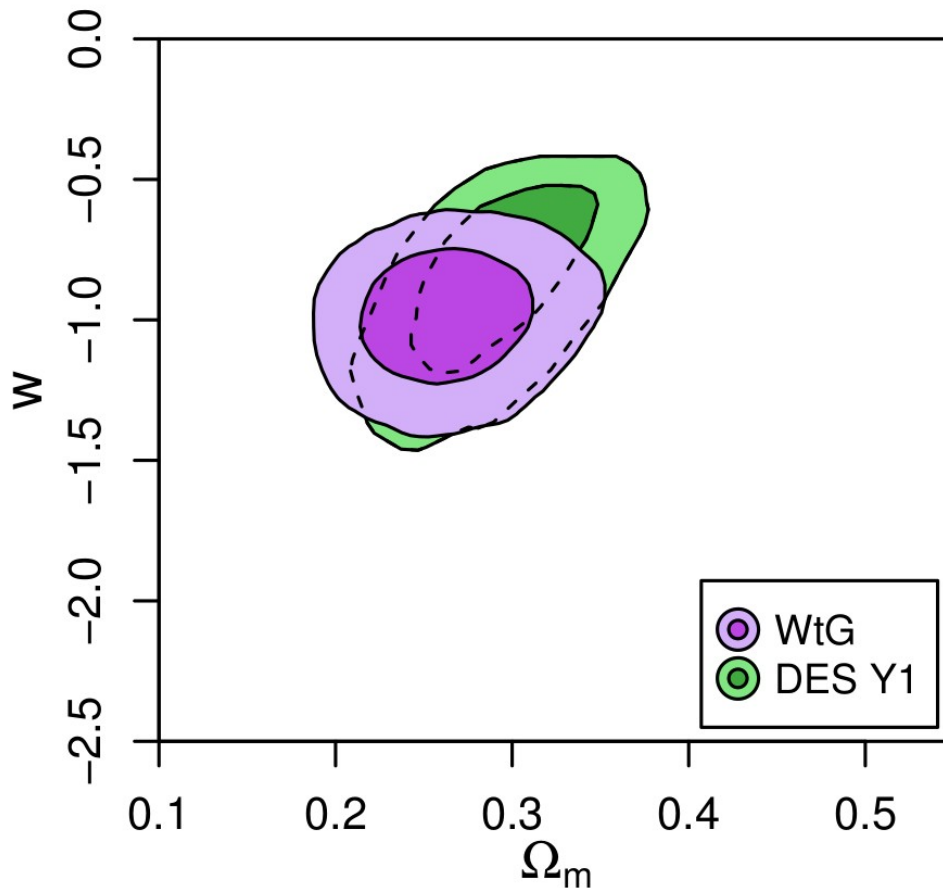
$$\Omega_m = 0.295 \pm 0.013$$

$$\sigma_8 = 0.819 \pm 0.026$$

$$w = -0.99 \pm 0.06$$

Cluster constraints from 224 massive clusters at $z < 0.5$ (+ Chandra X-ray + WTG weak lensing) competitive with other leading cosmological methods.

Comparison: X-ray clusters vs. DES Year 1



Flat, constant w model:

Clusters (Mantz et al. '15)

DES Y1 (Abbott et al. '12)

Note: DES Y1 constraint combines galaxy clustering and weak lensing (cosmic shear + galaxy-shear cross correlation).

Cluster constraints from 224 massive clusters at $z < 0.5$ (+ Chandra X-ray + WTG weak lensing) competitive with other leading cosmological methods.

The Road Ahead

Surveys on the near and mid-term horizons (2017-2023)

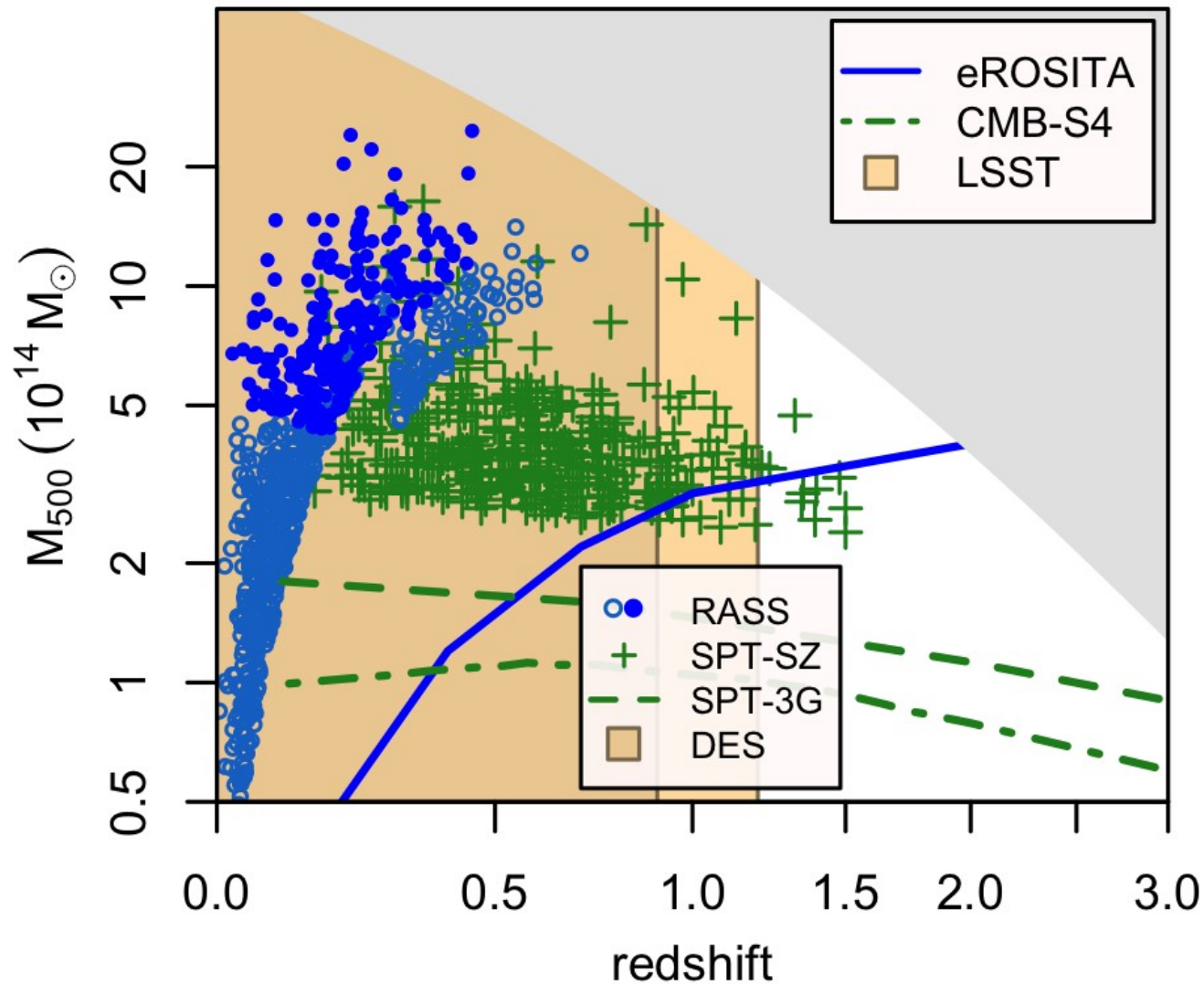


Projects: Optical/NIR: (DES, HSC), Euclid, LSST
mm: SPT3G, AdvACT/Simons Obs, CMB-S4
X-ray: eROSITA

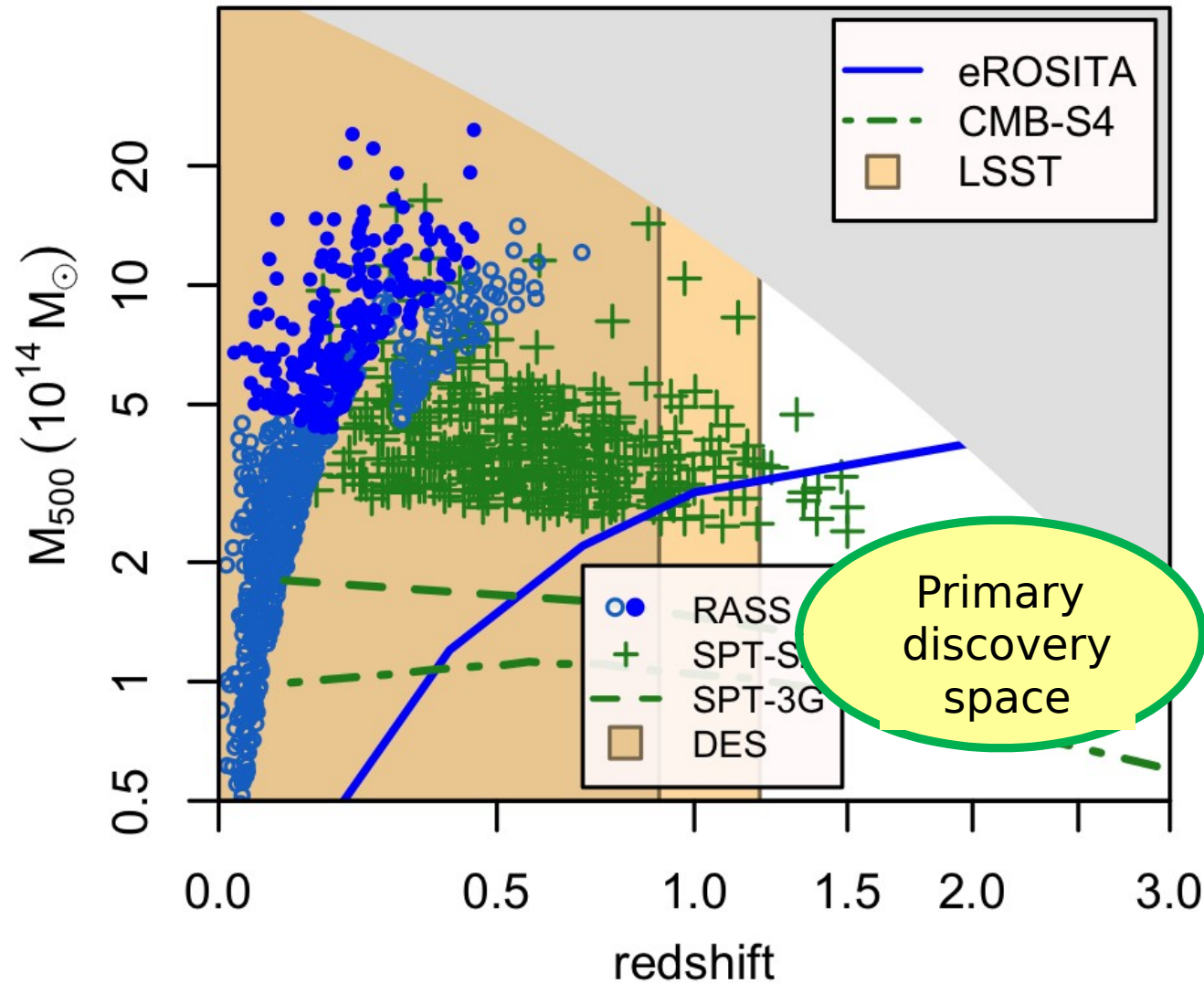
Strengths: Optical/NIR: cluster finding, photo-zs, WL mass cal.
mm: high-z cluster finding, CMB-WL mass cal.
X-ray: cluster finding, low-scatter mass proxies.

These projects are each powerful (finding 10^5 clusters) but also exceptionally synergistic: **far stronger in combination than alone.**

The discovery space of near and mid-term surveys

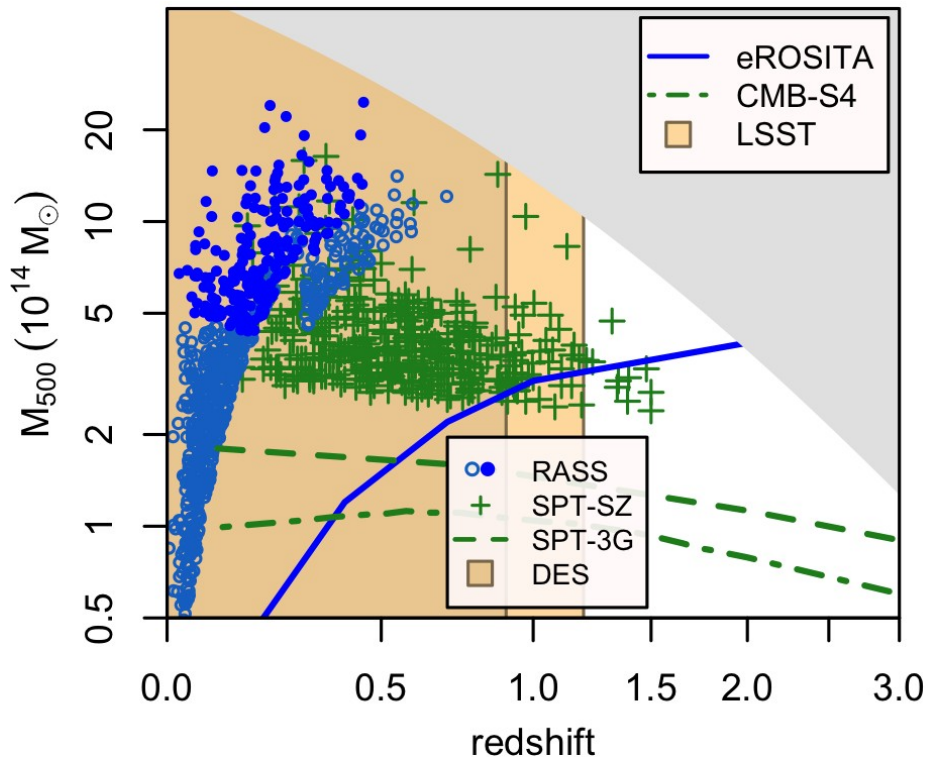


The discovery space of near and mid-term surveys



Exploiting these surveys for cosmology

Together mm-wave and optical/NIR surveys will trace cluster growth out to $z \sim 3$ (when massive clusters first formed) and provide precise photo- z 's + robust absolute mass calibration. X-ray follow-up measurements will be needed for precise **relative** mass calibration.



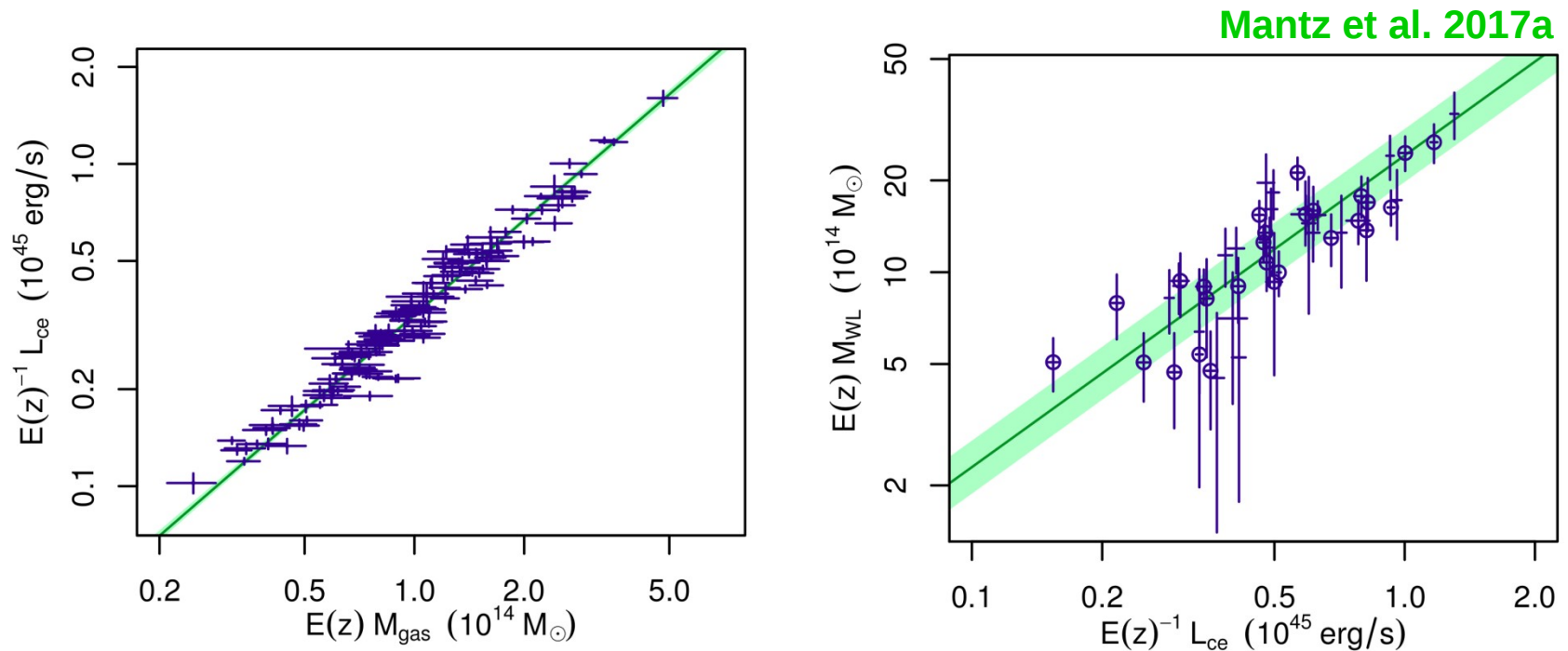
Ideally we would gather M_{gas} , T_x , Y_x for a representative subsample (few %) of clusters.

But gathering the necessary counts (1000-2000/target) is expensive (≥ 100 ks/cluster).

What can we do within a reasonable total Chandra + XMM-Newton budget?

A new low-cost mass proxy for cluster cosmology

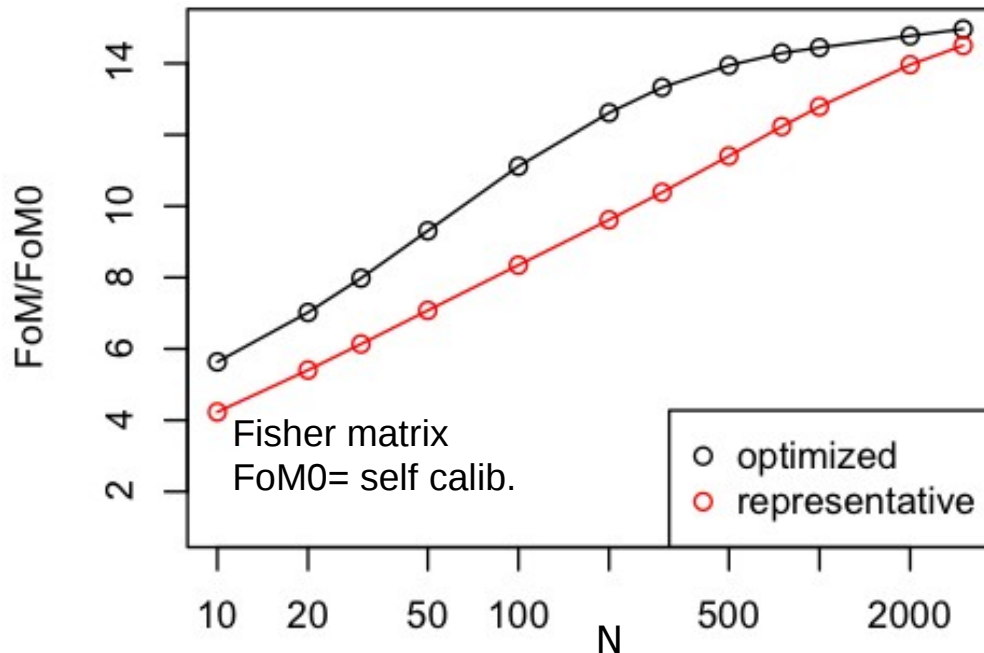
The center-excised X-ray luminosity, L_{ce} , can provide a 'cheap' (requiring only 100-200 counts to measure vs. 1000-2000 for M_{gas} , T_x , Y_x), low-scatter (<20%) mass proxy for massive clusters.



L_{ce} measurements can also be used to tune exposure times for deeper obs., e.g. to measure M_{gas} , T_x , Y_x + enable range of astrophysics.

How well could we do with such an approach?

Consider, e.g. follow-up of a 'Stage 3' CMB survey (~ 5000 clusters @ $z < 3$). Assume: Chandra + XMM-Newton investment of $3+3=6$ Ms over next 5 years \rightarrow Lce for ~ 150 clusters (Chandra) + Mgas, Tx, Yx for ~ 50 (XMM-Newton).



Fisher matrix forecast (Wu et al. 2010) of improvement in DETF FoM for SPT-3G-like survey as number of X-ray follow-up targets increases.

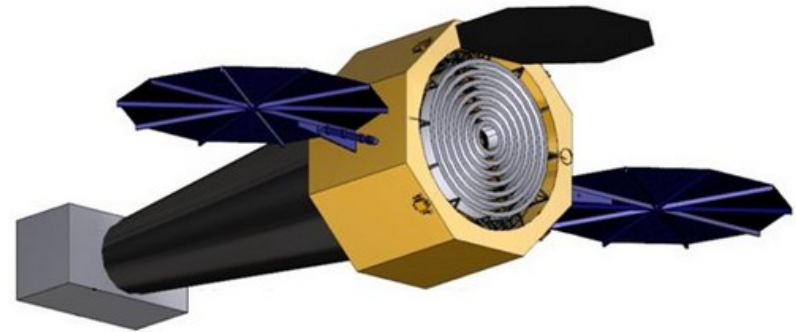
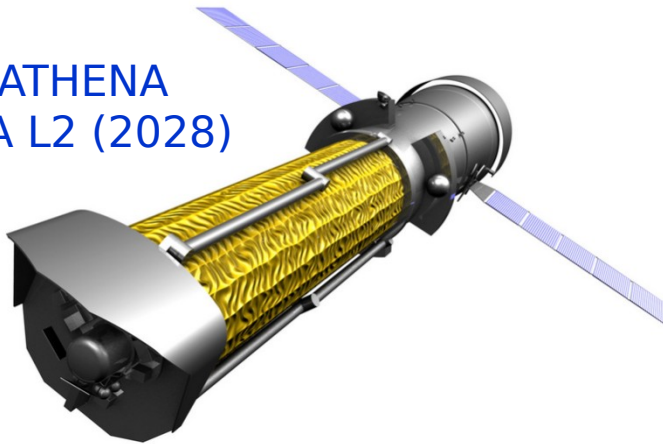
Targets can be optimized for a given question but should be somewhat representative.

This strategy can deliver order of magnitude gains in cosmological constraining power (and simultaneously address a range of astrophysics questions).

Next generation X-ray flagships

The full exploitation of `Stage 4' cluster surveys (e.g. LSST, CMB-S4) for cosmology and astrophysics will require new flagship X-ray observatories.

ATHENA
ESA L2 (2028)



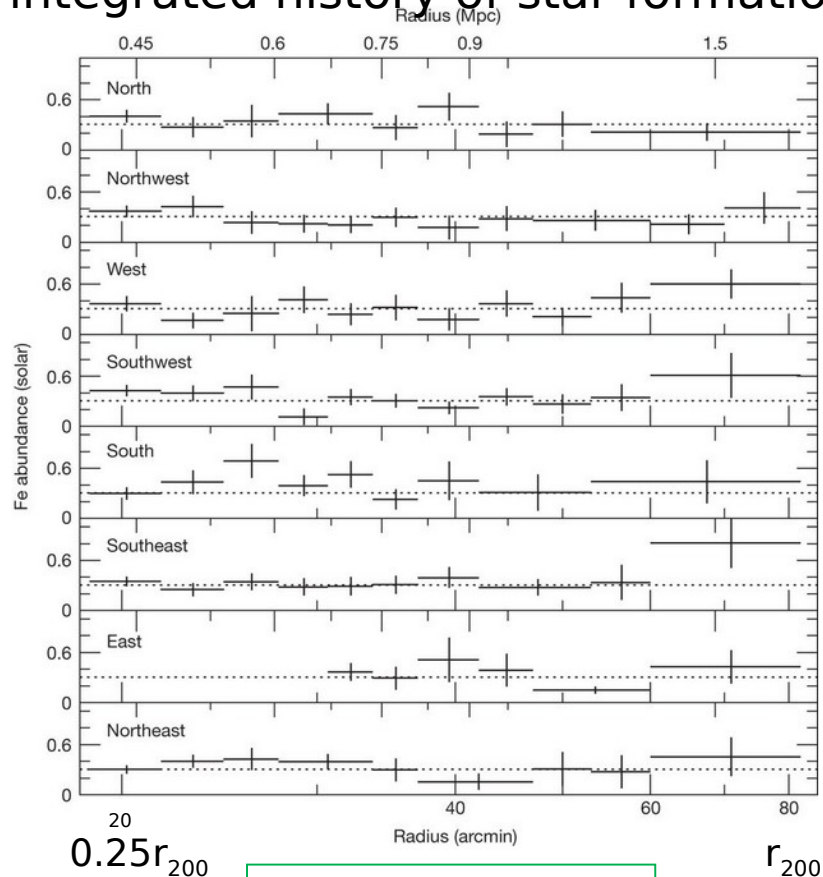
Lynx (under study for
2020 NRC Decadal Review)

Defining characteristics:

- Large collecting area ($\geq 50x$ Chandra)
- High quality imaging (5" HPD Athena, 0.5" HPD Lynx)
- Wide field imagers + large TES IFUs (+ gratings for Lynx)

The integrated history of star formation

The gravitational potential wells of clusters hold essentially all of the metals ever produced by stars in member galaxies → measurements of the metallicity of the ICM and its evolution strongly constrain the integrated history of star formation.



Werner et al. 2013

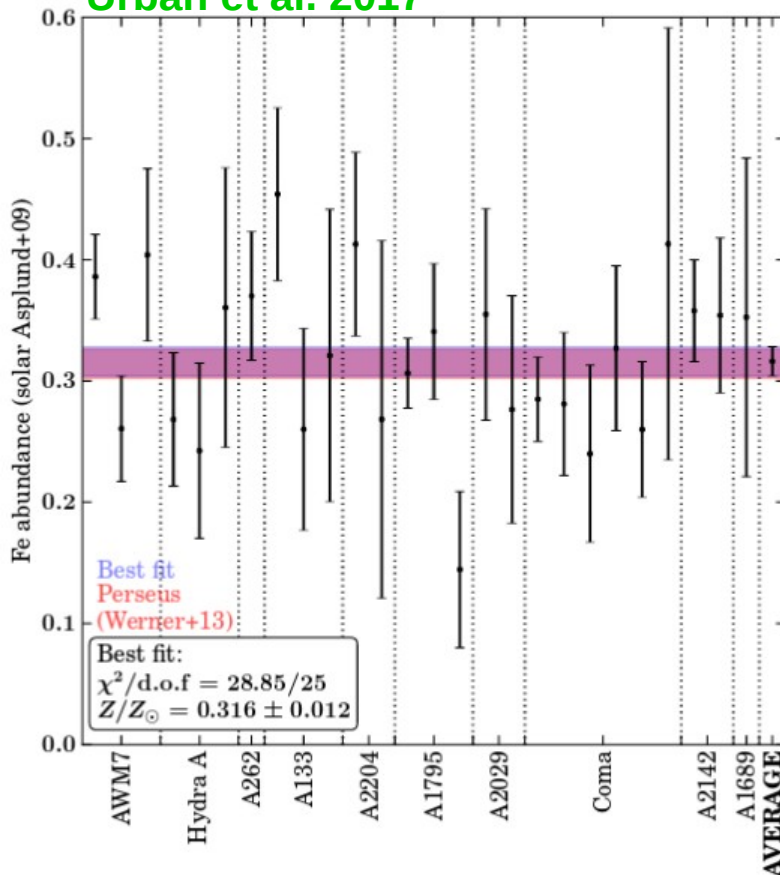
Suzaku measurements of a near uniform Fe abundance in the outskirts ($r > 0.25r_{200}$) of nearby clusters point to an early enrichment scenario, where the majority of IGM metal enrichment occurred before clusters formed

Perseus Cluster (76 regions)
 $Z_{\text{Fe}} = 0.314 \pm 0.012$ ($\chi^2 = 66/75$ dof)

The integrated history of star formation

The gravitational potential wells of clusters hold essentially all of the metals ever produced by stars in member galaxies → measurements of the metallicity of the ICM and its evolution strongly constrain how and when the IGM was enriched.

Urban et al. 2017



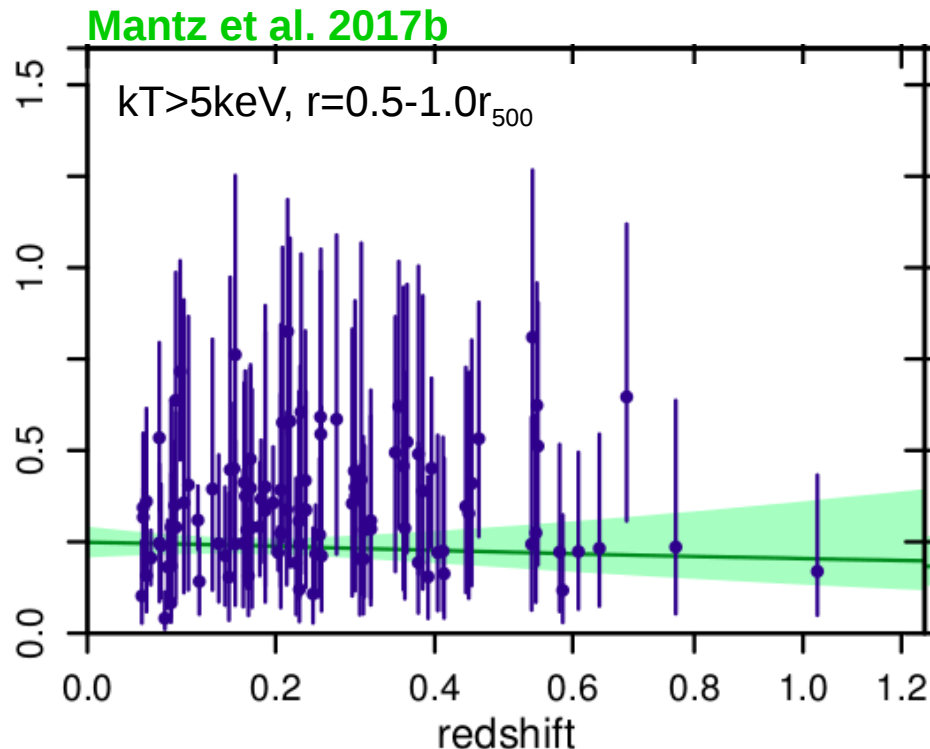
Suzaku measurements of a near uniform Fe abundance in the outskirts ($r > 0.25r_{200}$) of nearby clusters point to an early enrichment scenario, where the majority of IGM metal enrichment occurred before clusters formed

Perseus Cluster (76 regions)
 $Z_{\text{Fe}} = 0.314 \pm 0.012$ ($\chi^2 = 66/75$ dof)

10 additional clusters (26 regions)
 $Z_{\text{Fe}} = 0.316 \pm 0.012$ ($\chi^2 = 29/25$ dof)

The integrated history of star formation

Chandra and XMM-Newton measurements directly show an absence of evolution in metallicity at large radii in massive clusters since $z \sim 1$.



Parameterized model:

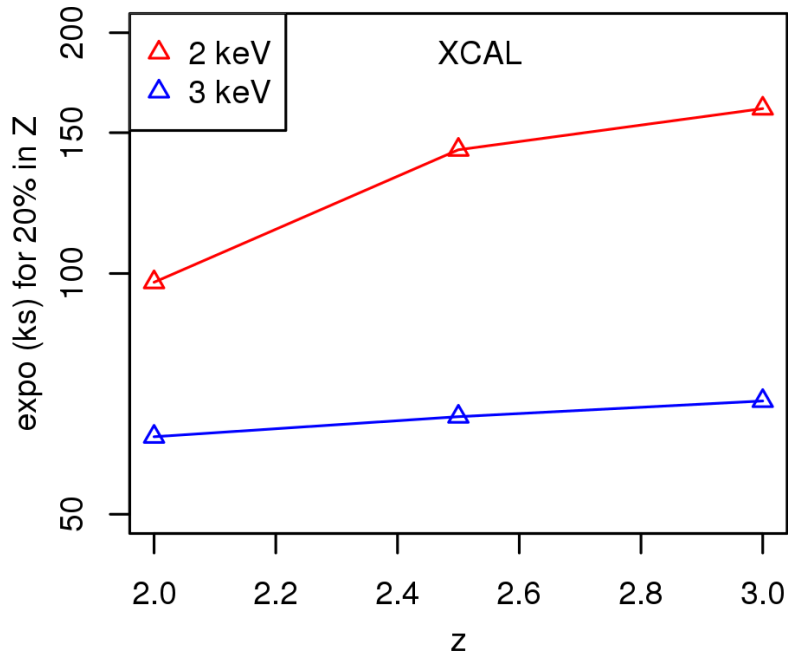
$$Z = Z_0 \left[\frac{1+z}{1+z_{piv}} \right]^\alpha \left[\frac{kT}{kT_{piv}} \right]^\beta$$

$$\alpha = -0.30 \pm 0.91, \beta = 0.22 \pm 0.34$$

See also consistent results from McDonald et al. 2016, Ettori et al. 2015,

Simulations tuned to match data observed metal distribution \rightarrow AGN winds were critical in driving early IGM enrichment (e.g. Biffi et al '17, Vogelsburger et al. '17).

Lynx and the integrated history of star formation



Key measurements:

- 1) AGN triggering in high-z clusters (see Noordeh talk)**
- 2) $Z(r,z)$ spanning epoch when star formation/AGN activity peaked and massive clusters first formed ($z=2-3$).**

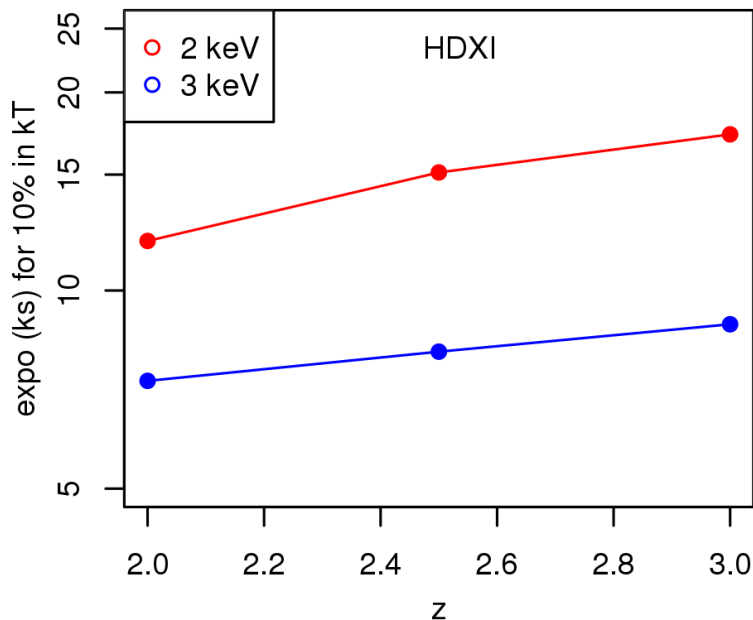
Synergies: CMB-S4, JWST, LSST, WFIRST, TMTs ...

Simulations → exposure requirements of ~ 60 ks per radial bin (~ 200 ks per target) for a 3keV cluster at $2 < z < 3$ to measure metallicity to 20% precision.

Observing a sufficient sample size (e.g. 10 clusters) to improve precision and probe system-to-system scatter → multiple Ms project.

Lynx and the fingerprints of feedback

Some of the clearest clues about the physics and impact of feedback processes are found in the thermodynamic properties of high- z groups and clusters.



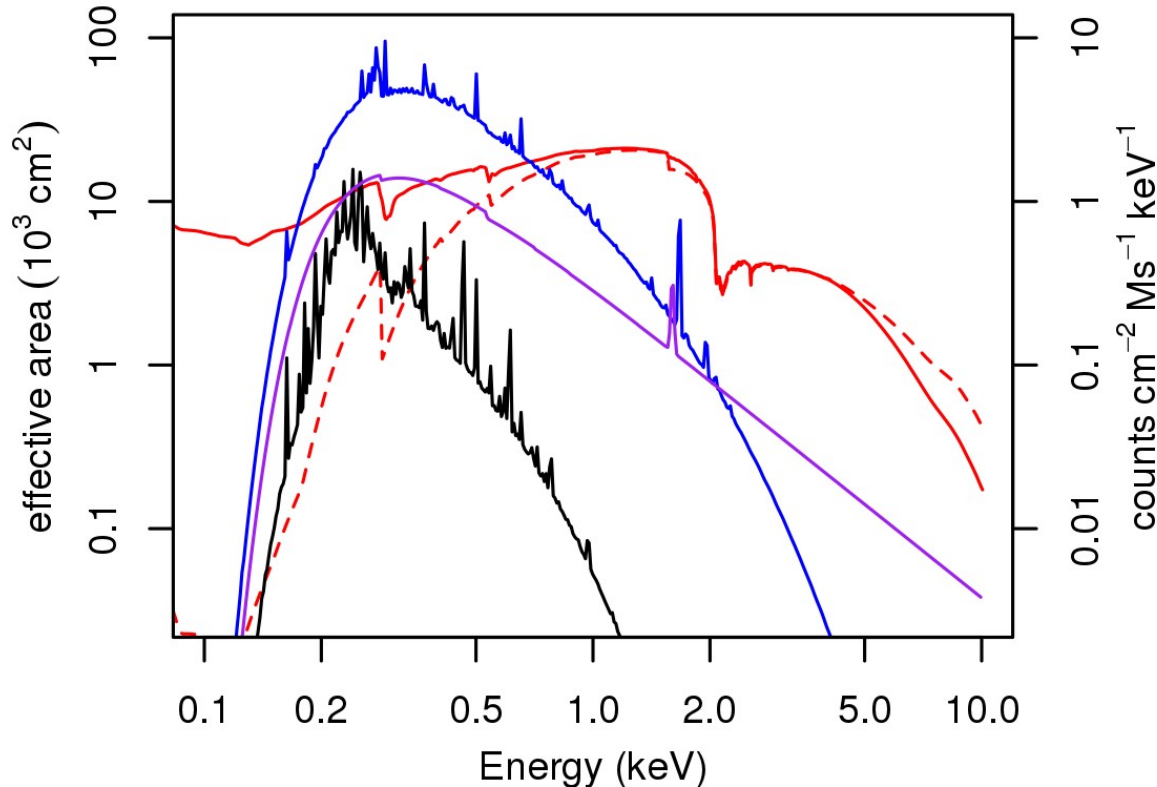
Key measurements:

- 1) AGN triggering in high- z clusters.**
- 2) Thermodynamic profiles spanning the epoch when star formation/AGN activity peaked and massive clusters first formed ($z=2-3$).**

Synergies: CMB-S4, JWST, LSST, SKA, WFIRST, TMTs ...

Simulations → exposure requirements of 5-20ks per bin (~ 100 ks per target) to measure thermodynamic properties to $\sim 10\%$ precision. Observing a sufficient sample size (e.g. 30 clusters) to probe system-to-system scatter → multiple Ms. (Note: observations will also serve broad range of other science).

The Lynx PSF and soft response are crucial



HDXI, XCAL ARFs

1 keV $z=3$ group
3 keV $z=3$ cluster
 $\Gamma=1.9$ $z=3$ AGN

All absorbed by
 $N_{\text{H}}=3\text{e}20/\text{cm}^2$

The enabling characteristics of Lynx for this science are its **high spatial resolution across large FOV** and **large effective area at soft energies**.

Conclusions

Measurements of cluster counts provide powerful cosmological constraints, competitive with the best other techniques.

The results on σ_8 and Ω_m from current X-ray/SZ/optical surveys agree well with each other (and with the primary CMB) when a consistent, rigorous mass calibration is adopted.

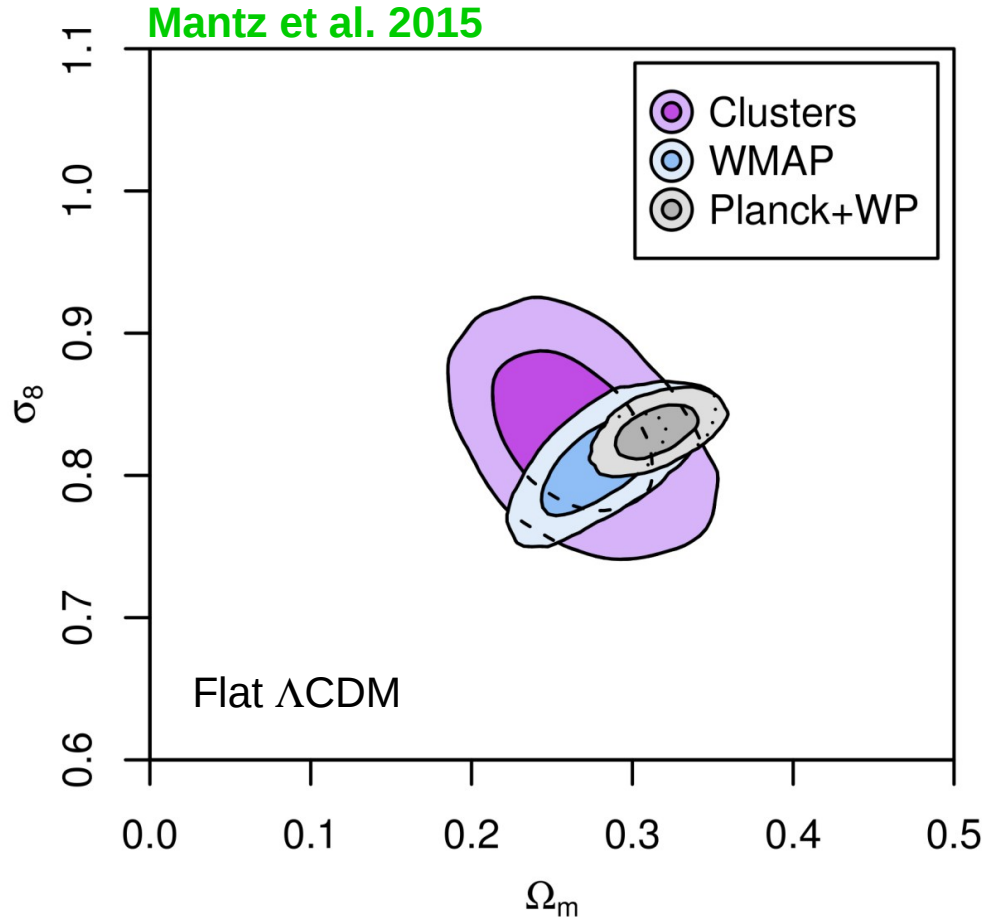
The prospects for rapid improvements using new, multi-wavelength surveys are outstanding. Coordinated analyses will be essential.

Reasonable investments of Chandra and XMM-Newton time over next 3-5 years could open up the potential of Stage 3 cluster surveys (e.g. SPT-3G, DES) for cluster astrophysics and cosmology.

Exploiting the full potential of Stage 4 surveys, however, will

Backup slides

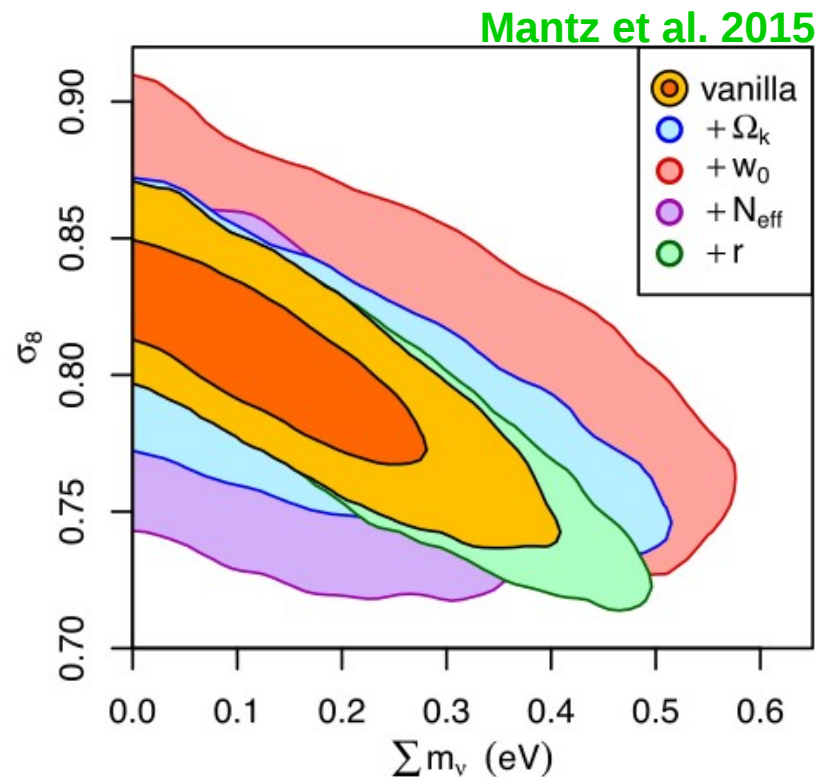
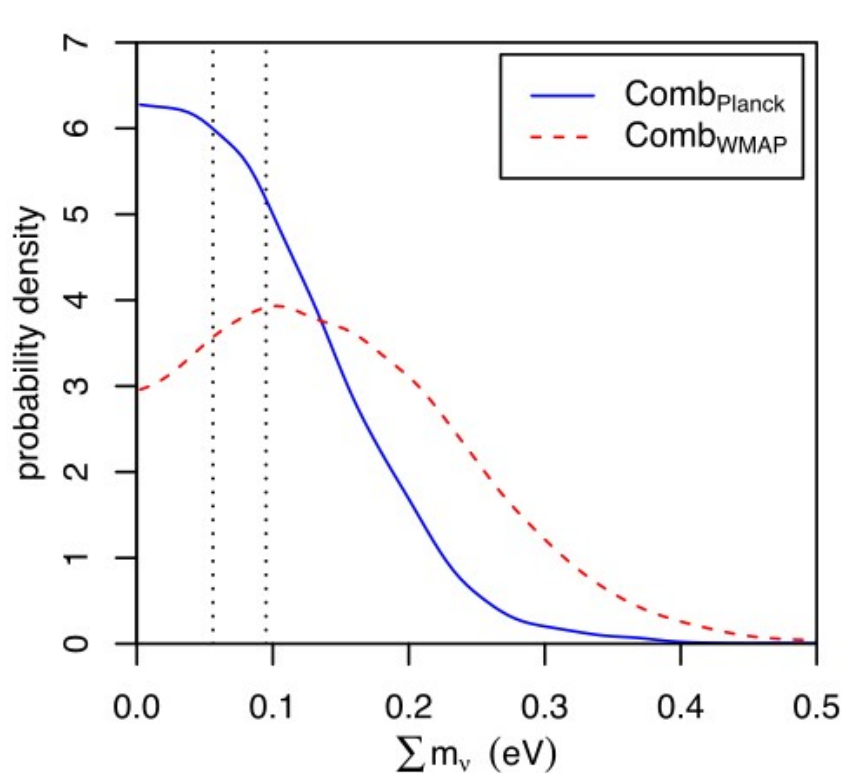
Current constraints: clusters vs. primary CMB



No tension between constraints from cluster counts and primary CMB (either WMAP or Planck) when employing full statistical framework and robust WL mass calib.

Current constraints: species-summed neutrino mass

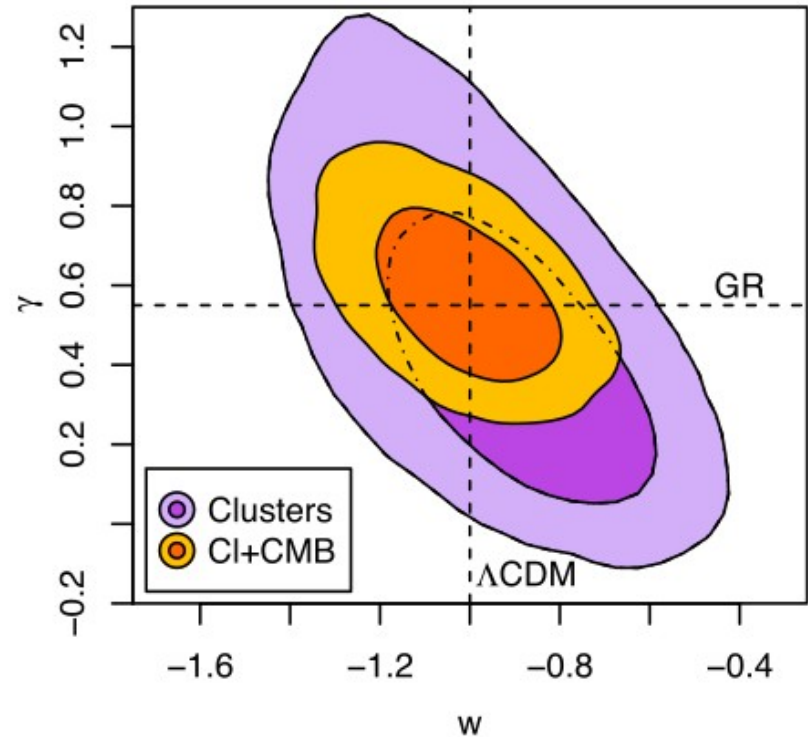
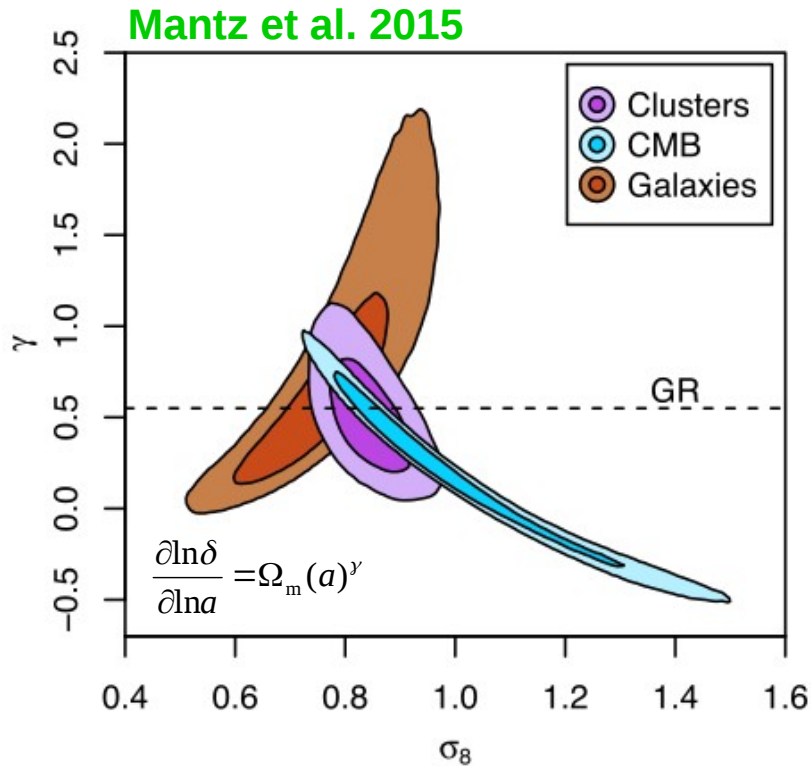
The inclusion of cluster count data leads to robust constraints on the species-summed neutrino mass.



For basic (flat Λ CDM) cosmology with no tensors:

$$M_\nu = \sum_i m_i < 0.22 \text{ eV (95\%)}$$

Current constraints: dark energy vs. modified gravity



Clusters also provide leading constraints on modified gravity models: results simultaneously consistent with GR + CC (see also e.g. Schmidt et al. '09, Rapetti et al. '10, '13; Cataneo et al. '15).

Enabling optical cluster cosmology

New optical surveys will deliver precise photo-zs and weak lensing constraints, and enable the construction of large cluster catalogs (see Rozo talk).

However, to fully enable optical cluster cosmology, two key systematics in catalog construction must be controlled at % level

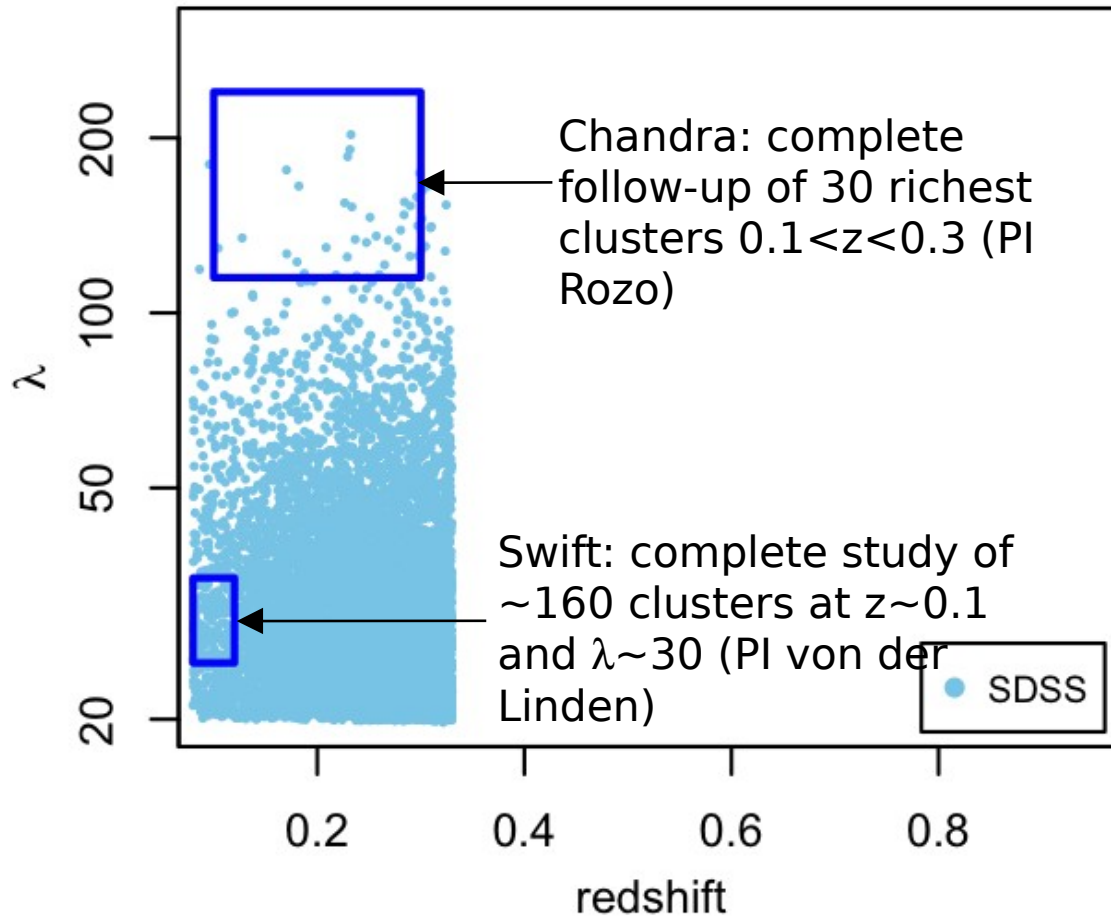
- Projection effects (systematic boosts in richness)
- Offsets between optical (BCG) and true halo centers.

Follow-up X-ray observations can address both concerns:

- Only virialized halos shine in X-rays → reveals projection effects
- X-ray emission traces 3D potential → robust centers.

By observing representative samples of optically selected clusters, we can build statistical models for both effects (as function of M, z) and fold into analysis.

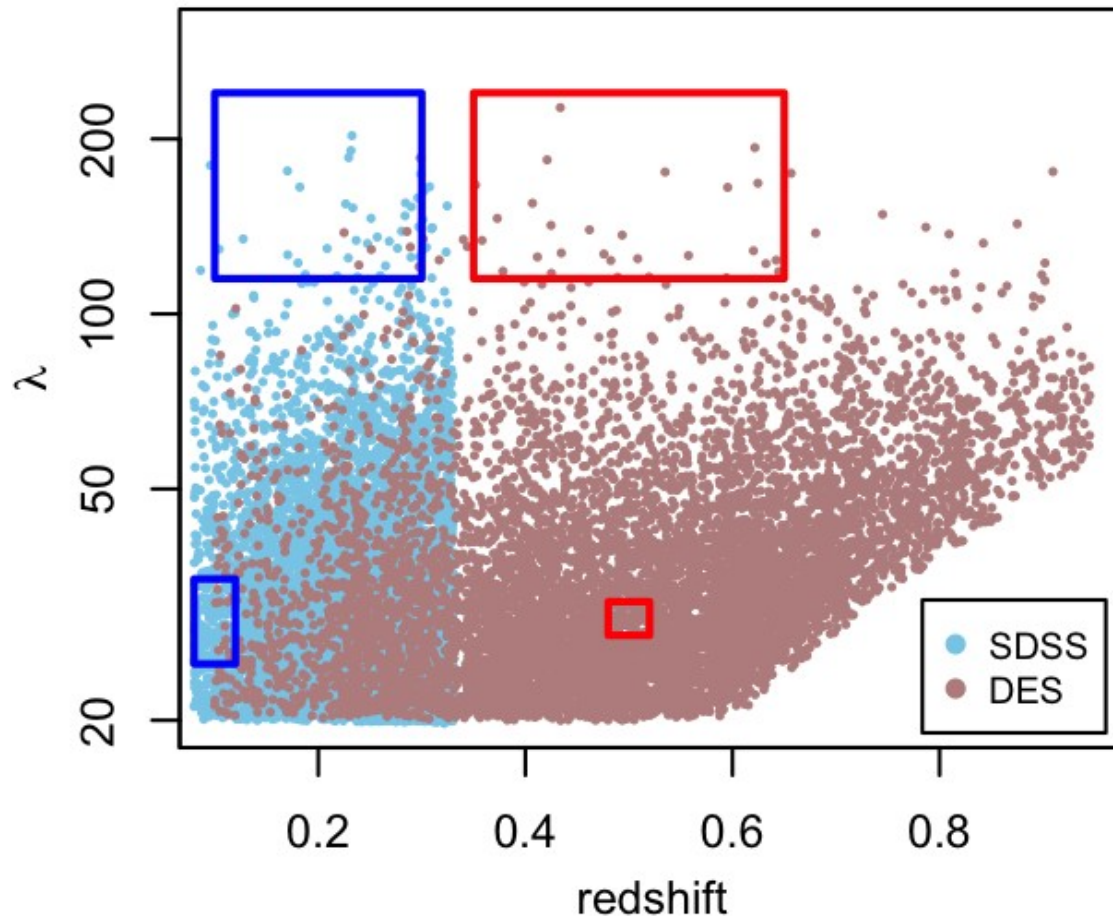
X-ray follow-up of optically selected clusters



**SDSS redMaPPer
cosmology catalog
(Rykoff)**

2 X-ray follow-up
programs underway
(data in hand). See
Mantz, Rozo talks.

X-ray follow-up of optically selected clusters



**SDSS redMaPPer
cosmology catalog
(Rykoff)**

2 X-ray follow-up
programs underway
(data gathered). See
Mantz, Rozo talks.

**Illustrative DES
catalog**

Similar X-ray follow-up programs will be required to fully enable DES cluster cosmology. This will likely require a legacy class XMM-Newton program.